UNRAVELING BIDIRECTIONAL CONVERTER CAPABILITIES: A DIDACTIC PLATFORM FOR PROVING DUAL-DIRECTION OPERATION BASED ON CURRENT INJECTION

Fabiano Gonzales Nimitti[1], António Manuel Santos Spencer Andrade[1,2]
[1]Federal University of Santa Maria, Santa Maria – RS, Brazil
[2]Federal University of Rio Grande do Sul, Porto Alegre – RS, Brazil
e-mail: fabianonimitti@gmail.com, antoniom.spencer@gmail.com

***Abstract* – In recent years, due to the exponential increase in the use of electric vehicles and microgrids, many studies have been conducted on bidirectional converters. However, laboratories are not always able to validate the bidirectionality results due to cost and complexity. Then, in this paper a new didactic platform to prove the bidirectional power flux in bidirectional power converters is presented. This platform works alongside with the control system to ensure a current injection and guarantee the power flux reversion in bidirectional converters. Besides that, also are presented the principle of operation, control system, mathematical modeling and instrumentation system. Finally, to validate the theoretical analysis the simulation and experimental results are presented proving the bidirectionality of two power converters working in 500 W.**

***Keywords* – Bidirectional, Converter, Reversion.**

NOMENCLATURE

V_L	Low voltage bus.
V_H	High voltage bus.
R_H	Resistance load.
D_{aux}	Auxiliary diode.
R_{aux_i}	Auxiliary resistance.
S_{aux}	Auxiliary switch.
V_{aux}	Auxiliary voltage source.
v_{gsaux}	Gate-Source voltage.
i_x	Current through an element x.
$C_x(s)$	Transfer function of a compensator x.
$H_x(s)$	Transfer function of a x sensor.
$\hat{i}_L(s)$	Inductor current transfer function.
$\hat{v}_h(s)$	High voltage side transfer function.
$\hat{d}(s)$	Duty cycle transfer function.
K_x	Gain x.
CCL	Current control loop.
VCL	Voltage control loop.
DSP	Digital signal processor.
A/D	Analog-to-Digital converter.
F_s	Switching frequency.
s	Complex analog variable.
z	Digital complex variable.
Ta	A/D converter sampling period.

Manuscript received 06/29/2023; first revision 08/11/2023; accepted for publication 10/19/2023, by recommendation of Associate Editor Heverton Pereira. http://dx.doi.org/10.18618/REP.2023.4.0020.

I. INTRODUCTION

In the last few years, due to the increasing number of devices connected to renewable and clean energy sources, the use of DC-DC bidirectional power converters has been growing exponentially [1]–[3]. The bidirectional nature of these converters allows for power flow in two directions: from the energy source to the storage system (charging mode) and from the storage system back to the source (discharging mode). This bidirectional functionality is essential in various applications, including electric vehicles, uninterruptible power sources and microgrids, as it facilitates energy management, power quality control, and grid integration [4]–[6].

In electric vehicles, bidirectional converters are essential for ensuring efficient energy transfer between the vehicle's battery and electric devices. They enable the conversion of stored energy in the battery to power the motors and supply energy to the vehicle's electrical systems. Additionally, during deceleration or braking, bidirectional converters allow the recovery of generated kinetic energy [7], converting it back into electrical energy and directing it back to the battery, thereby helping to extend the vehicle's autonomy.

In the context of uninterruptible power sources, bidirectional converters are used to provide continuous and reliable power during electricity outages [8], [9]. They allow the energy stored in storage systems, such as batteries or capacitor banks, to be converted and made available to power critical devices during grid disruptions. This ensures that essential equipment and systems can continue operating without interruption, even when there is a lack of grid power.

Furthermore, in the realm of DC microgrids, bidirectional converters play a fundamental role in the efficient distribution of power in DC systems [10],[11]. They enable the connection of storage systems to the DC bus, where they can provide power during intermittent periods of renewable energy sources or be used to recharge the storage system during excess energy availability.

Among bidirectional converters, there are two main classes: non-isolated and isolated converters. Non-isolated converters [12]–[14], which are more commonly used in uninterruptible power sources, offer higher efficiency, lower costs, smaller volumes, and reduced voltage stresses. However, their voltage gain is closely tied to the chosen topology. Isolated converters [15]–[17] are the most used in electric vehicles

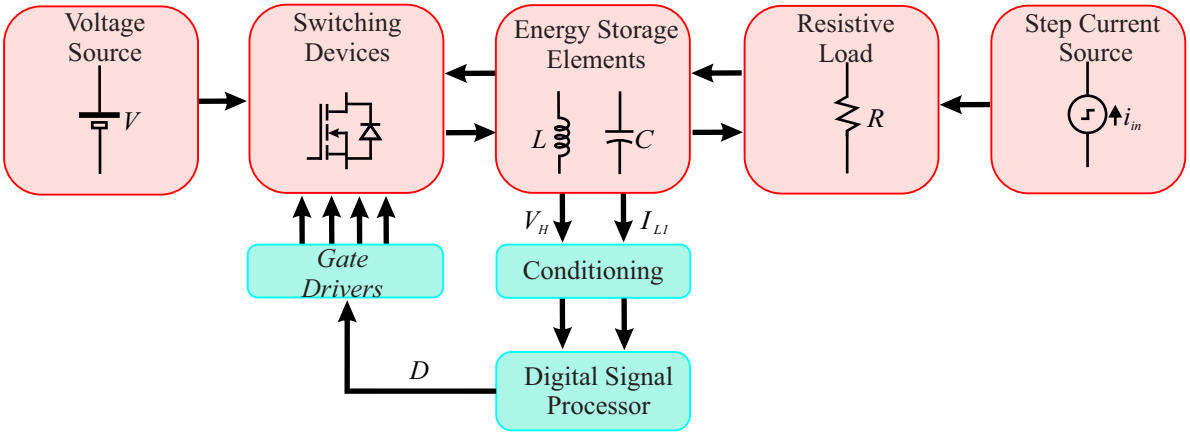

Fig. 1. Hardware Solution

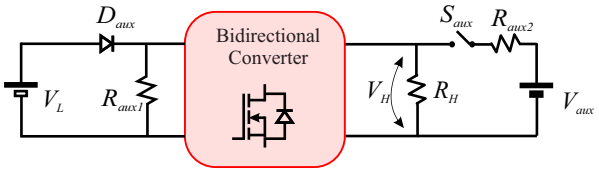

Fig. 2. Simplified Hardware Solution

and microgrid applications, it employ galvanic isolation using a high frequency transformer or coupled inductor to ensure the safety of connections between high and low voltage buses. However, these magnetic devices incur energy losses from core magnetization and copper resistance. Moreover, these converter can achieve high voltage gain adjusting the transformer turn ratio, but due to their high number of magnetic elements, isolated converters experience voltage spikes caused by the discharge of parasitic inductance in the windings. Moreover, isolated bidirectional topologies may present problems by zero crossing of the inductors current and hence are not be able to invert the power flux in online operation, being necessary a demagnetization switch to restart the converter [18], which takes time and energy dissipation.

Given the characteristic and application of the bidirectional converters, is notable that a converter that does not require a restart to change power flow is highly desirable as it consumes less time and wastes less energy. To achieve this, is necessary to prove the capability of online power flow change. The better way to reach it is using two bidirectional power supplies in each voltage bus, but these sources are expensive and very difficult to find suppliers for higher powers.

The papers do not make clear how to perform bidirectionality tests, or sometimes do not even demonstrate such results. This way, it become a challenge for new researchers, given the lack of dissemination of this information.So, numerous researchers have been seeking to simulate the real operating conditions of their applications using didactic platforms. In [19], a method is introduced for assessing control strategies applied to power electronics and motors, aiming to alleviate both generation and motorization issues. For a better grasp of motor drivers, [20] details the development of a driver for DC motors. [21]–[23] offer a simplified approach to understanding various switched converters. In the field of mechanical engineering, [24] evaluates a teaching platform designed for instructing students on transmission gears in hybrid vehicles. These approaches has demonstrated increased speed and reduced costs in obtaining practical results, given that with the didactic platforms, there is no longer a need for real-world application.

So, in order to obtain a simple and low cost way to prove the online bidirectionlity this paper present a new platform based on current injection performed by a step current load controlled by a control system. The complete system is shown in Figure 1, where is possible to see the V_L and V_H voltage buses, the bidirectional converter (represented by the switching devices, energy storage elements and resistive load) and the step current load.

To demonstrate the advantages, disadvantages, and limitations of the proposed didactic platform, in this paper are presented the conditions for a converter to be bidirectional, in Section II. In Section III, the principle of operation. In the Section IV the design methodology is presented. In Section V the modeling and control system are done. In Section VI, the instrumentation system is presented. To finalize, Section VII and VIII demonstrate the simulation and experimental results, respectively, while the main conclusion of this paper are presented in Section IX.

II. CONDITION FOR A CONVERTER TO BE BIDIRECTIONAL

The power converters present different characteristics among them, some of which are necessary and desirable to prove the converters' bidirectional nature. Therefore, in this section, the conditions for a converter to be bidirectional will be presented based on [25]. Below are listed these conditions:

1. Can not present diodes in its topologies, as this device only allows the current travel in one direction;
2. The inductor must have a path to charge/discharge or free-wheeling path in every operation stage.
3. Its topology must work in the four quadrants of the voltage-current curve;

Regarding item 1, a visual inspection is necessary to evaluate the presence of diodes in the topology. In connection with item 2, the converter's stage of operation must be known to understand the current paths. Meanwhile, item 3 can be proven using the proposed platform to invert the power flux

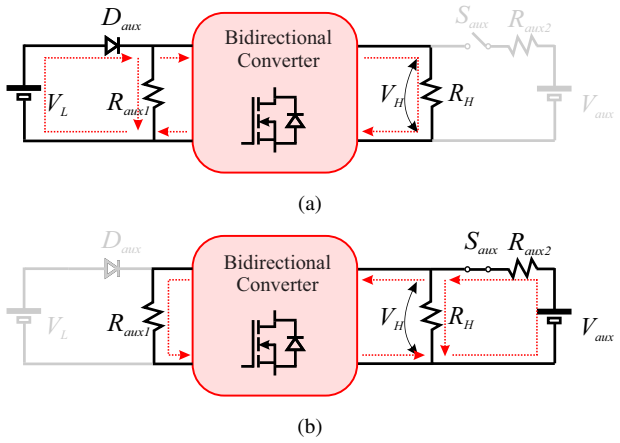

Fig. 3. Hardware Stages of Operation. (a) Stage I. (b) Stage II.

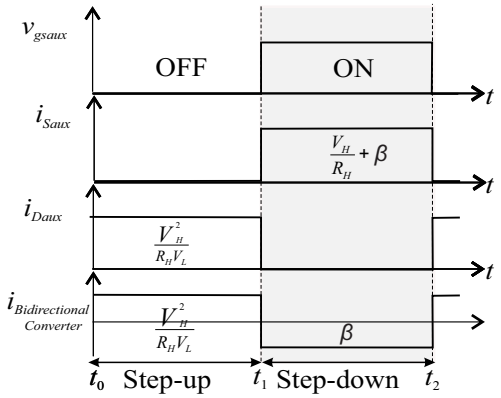

Fig. 4. Theoretical Waveforms.

while keeping the voltages stable.

III. PRINCIPLE OF HARDWARE OPERATION

As there is no way to implement ideal current sources, it is realized using a voltage source in series with a resistor, as shown in Figure 2. The hardware consists of 3 resistors, 2 voltage sources, 1 diode, and 1 switch. Furthermore, at this moment, the bidirectional converter is treated as a black box for better understanding. Examples with real bidirectional converters are provided in the case studies in Sections VII and VIII. This technique consist in current injection by a step current source in a way to feed the load. The current excess is driven by the bidirectional converter, changing the current flux direction.

This approach present two stage of operation, in the first the converter is operating in step-up mode, while in the second a current is injected to invert the power flux. These stages are presented in Figure 3, while in Figure 4 its main waveforms are depicted,where V_{gsaux} represent the gate-source switch voltage; i_{Saux} is the current passing through the switch S_{aux}; i_{Daux} is the current passing through the diode D_{aux} and $i_{BidirectionalConverter}$ is used to represent the current passing through the bidirectional converter.

A. Principle of Operation

Stage I [Figure 3.a, $t_0 - t_1$]: During this stage, the power converter initiates its step-up operation, the power flow from V_L to V_H. The switch S_{aux} remains OFF, resulting in a current

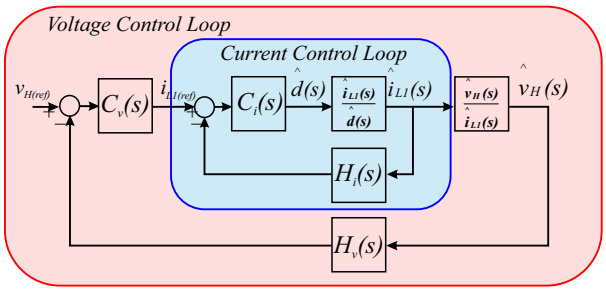

Fig. 5. Control Strategy.

defined as:

$$i_{Saux} = 0. \tag{1}$$

Stage II [Figure 3.b, $t_1 - t_2$]: During this stage, the switch S_{aux} is activated, causing a current to be introduced into the V_H bus. A portion of this current is consumed by the resistor R_H, while any excess current is directed through the power converter and dissipated across R_{aux1}. As a result, this process reverses the power flow, inducing the power converter to enter a step-down mode. Besides that, to prevent damage from reverse currents in the V_L source, the auxiliary diode goes into blocking state.

$$i_{Saux} = \frac{V_{aux} - V_H}{R_{aux2}}. \tag{2}$$

IV. DESIGN METHODOLOGY

To find the value of the resistance R_{aux2}, is necessary set a value for V_{aux} and then determine the value of R_{aux2} such that the current injected by V_{aux} must be sufficient to feed the load R_H and have a surplus (β) for the converter to drain and reverse the current direction, as shown in (3).

$$i_{Saux} = \frac{V_H}{R_H} + \beta. \tag{3}$$

Rearranging (3) with (2), the resistance R_{aux2} is presented in (4).

$$R_{aux2} = \frac{V_{aux} - V_H}{\frac{V_H}{R_H} + \beta}. \tag{4}$$

The resistance R_{aux1} is calculated based on the power drained by the converter. This power is given by (5), where ideally, the power drained from the V_H side should be the same as the power injected to the V_L side and must be absorbed by R_{aux1}.

$$P_H = P_L = P_{Raux1} = V_H \beta. \tag{5}$$

Rearranging (5) and applying the power formula for a resistor, is presented the value of the resistance R_{aux1} in (6).

$$R_{aux1} = \frac{V_L^2}{V_H \beta}. \tag{6}$$

V. CONTROL STRATEGY

When the platform injects current, there is an excess of power on the V_H side. In this situation, the converter must adjust its operating point to ensure that this excess power is drained properly. Otherwise, this surplus power will be absorbed by the converter's capacitor, leading to an increase

in the voltage level of V_H. In this sense, to solve this problem, the hardware solution presented need to work along side with a control system. Therefore, in an attempt to correct it, the control system updates the converter duty cycle and hence drain the excess of current.

As the main objective of this platform is keep the voltage V_H stable and allow the online power flux changing, a dual loop control system is required, as show in Figure 5. The internal loop control the current through the inductor, as to prove the bidirectionality it must present zero crossing. The external loop control the voltage V_H and generate a current reference to the internal loop.

A. Mathematical Modeling

The power converters presented and detailed in [26], [27] and depicted in Figure 6 are used to evaluate the proposed platform. According to the respective references, both converters have the same state-space dynamic model, as shown in (7).

$$\begin{bmatrix} \dot{v}_H \\ \dot{i}_{L1} \end{bmatrix} = \begin{bmatrix} -\frac{1}{R_H C_H} & -\frac{D-1}{C_H} \\ \frac{D-1}{2L_1} & 0 \end{bmatrix} \begin{bmatrix} v_H \\ i_{L1} \end{bmatrix} + \begin{bmatrix} 0 \\ \frac{1}{2L_1} \end{bmatrix} V_L. \tag{7}$$

Since the state space technique exhibits nonlinear characteristics, a linearization process becomes necessary to derive linear transfer functions. This procedure, commonly referred to as "disturb and linearize" [25], involves representing all state space variables ($x(t)$) as a combination of static gains (X, V_L, and D) and small time-varying disturbances ($\hat{x}(t)$, $\hat{v_L}(t)$, and $\hat{d}(t)$). This transformation is demonstrated in (8-10). Following the disturb and linearize process, the nonlinear terms can be disregarded, and the Laplace transform can then be applied to derive the linear transfer functions.

$$x(t) = X + \hat{x}(t) \tag{8}$$

$$v_L(t) = V_L + \hat{v_L}(t) \tag{9}$$

$$d(t) = D + \hat{d}(t). \tag{10}$$

Considering the parameters given in Table I, the transfer functions are are given by:

$$\frac{\hat{v_H}(s)}{\hat{d}(s)} = \frac{\alpha_1 s + \alpha_2}{s^2 + \beta_1 s + \beta_2} \tag{11}$$

$$\frac{\hat{i_{L1}}(s)}{\hat{d}(s)} = \frac{\delta_1 s + \delta_2}{s^2 + \beta_1 s + \beta_2} \tag{12}$$

$$\frac{\hat{v_H}(s)}{\hat{i_{L1}}(s)} = \frac{\alpha_1 s + \alpha_2}{\delta_1 s + \delta_2} \tag{13}$$

where $\alpha_1 = -1.478E4$, $\alpha_2 = 5.674E8$, $\delta_1 = 7.407E5$, $\delta_2 = 5.597E-6$, $\beta_1 = 13.3$, $\beta_2 = -5.106E5$.

B. Control Design

The proportional integral (PI) controllers was designed using MATLAB's Sisotool and the Bode diagram, with the zeros, poles, and gains of the controller tuned to achieve a low crossover frequency in order to minimize low-frequency oscillations during transients. The PI controllers are

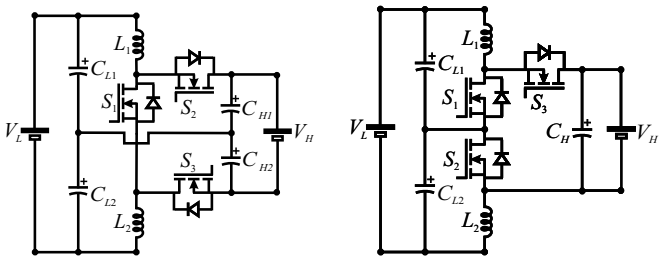

Fig. 6. Converters used to evaluate the platform. (a) Converter [26]. (b) Converter [27].

Fig. 7. Bode diagram for voltage V_H loop.

represented as follows:

$$C_v(s) = \frac{0.8237s + 41.18}{s} \tag{14}$$

$$C_i(s) = \frac{0.007489s + 23.53}{s}. \tag{15}$$

Figure 7 displays the Bode diagram for both the compensated and uncompensated V_H system. The PI controller attains an impressive phase margin of 86° at 100 Hz and a substantial gain margin of 29.44 dB at 1677 Hz, effectively achieving the desired performance objectives, as detailed in the simulation and experimental results section.

C. Digitization Technique

An optimal approach to implementing digital control involves utilizing the Zero-Order Hold (ZOH) and Unity Delay model methods to represent the ADC and unity delay, respectively. These models typically incorporate a low-pass filter with a high cutoff frequency. However, in this paper, is adopted lower cutoff frequencies in order to ignore these effects.

To digitally implement the control system, a digitization step is required. The chosen step is known as the Tustin technique or trapezoidal method. This technique approximates the integral by mapping the area under the function in the "s" plane using infinite trapezoids. Among all the discretization techniques, this one provides an exact mapping between the analog "s" plane and the digital "z" plane [28]. To apply this technique, you simply replace the "s" in the transfer function of the compensators with (16). The inverse transformation is

TABLE I
Converters Parameters

Parameter	Value
Output Power	500 W
High Side Voltage V_H	400 V
Low Side Voltage V_L	144 V
Switching frequency F_s	50 kHz
Converters Switches	IRFP4868
Gate Driver	IR2110
Converters Inductors L_1 and L_2	270 μH @ 0.4Ω
Converters Capacitors C_{H1}, C_{L1} and C_{L2}	470 μF

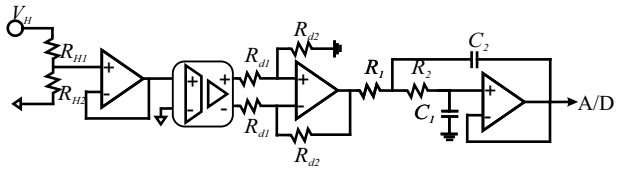

(a)

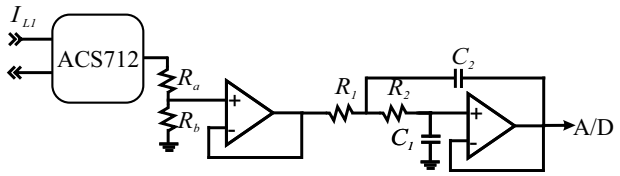

(b)

Fig. 8. Instrumentation System of (a) V_H Voltage. (b) Inductor Current.

also possible by replacing the "z" with (17).

$$s = \frac{2(z-1)}{Ta(z+1)} \tag{16}$$

$$z = \frac{2+sTa}{2-sTa}. \tag{17}$$

VI. INSTRUMENTATION SYSTEM

Since the control system operates digitally, an instrumentation system is necessary to acquire and condition the control signals to levels compatible with the digital signal processor. This system is constructed using operational amplifier techniques [29].

A. Voltage Sensor

In Figure 8.a is shown the voltage sensor. It is performed by a resistive divisor to decrease the signal amplitude, followed by a voltage buffer to match the impedance. The resulting voltage gain is given by (18).

$$K_{VH} = \frac{R_{H2}}{R_{H1}+R_{H2}}. \tag{18}$$

To achieve isolation between the DSP and the power converter, the next stage employs an isolated operational amplifier (HCPL-7840). This operational amplifier can handle a maximum voltage of 0.2V and provides a voltage gain of 8 times at its differential output.

To convert its differential output into a single output, a differential operational amplifier is utilized, and the voltage gain of this circuit is determined by (19).

$$\frac{V_{dif}}{V_a - V_b} = K_{dif} = \frac{R_{d2}}{R_{d1}}. \tag{19}$$

Finally to eliminate the switching noises, an anti-aliasing second order low pass filter is used. Normally, its cut-off frequency is around one decade below of the A/D sampling frequency. This transfer function is given in (20).

$$\frac{V_o(s)}{V_{in}(s)} = \frac{\frac{1}{R_1R_2C_1C_2}}{s^2 + \left(\frac{1}{R_1C_2} + \frac{1}{R_2C_2}\right)s + \frac{1}{R_1R_2C_1C_2}}. \tag{20}$$

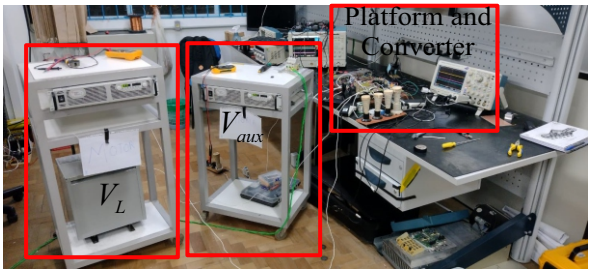

Fig. 9. Practical setup.

B. Current Sensor

Because of the bidirectional nature of the proposed platform, it is necessary to employ a sensor capable of measuring current in both directions. To fulfill this requirement, the ACS-712 sensor is utilized, as depicted in Figure 8.b. This sensor provides galvanic isolation between the power converter and the DSP. To adjust the output level to the DSP's requirements, a resistive divider is employed, followed by a voltage buffer to match the impedance. Finally, the same filter as described in (20) is used as an anti-aliasing filter. The gain of the resistive divider is demonstrated in (21).

$$K_{IL} = \frac{R_b}{R_a + R_b}. \tag{21}$$

VII. SIMULATION RESULTS

To gain a deeper understanding of the power flux reversal approach, simulations were conducted on the converters depicted in Figure 6. These simulations were carried out under power flux reversal conditions, utilizing the parameters listed in Table I and Table II. The simulation results are presented in Figure 10, with the first moment involving a transition from step-up to step-down, and the second moment from step-down to step-up. These results clearly demonstrate the zero crossing of the inductor current without any adverse effects on the voltage V_H, thereby confirming the bidirectional capability of the mentioned converters.

VIII. EXPERIMENTAL RESULTS

To evaluate the accuracy of theoretical evaluations, a prototype of the proposed inversion platform was built in the laboratory, as showed in Figure 9. The converters used for validation are well known and presented in Figure 6, while its specification are given in Table I and Table II. To create V_L and V_{aux}, a Keysight N8762A DC voltage source was used. To digitally run the control strategy and generate the PWM signal, a STM32F411 Digital Signal Processor was used.

TABLE II
Platform parameters

Parameter	Value	Parameter	Value
V_{aux}	430 V	R_{H2}	400 Ω
R_{aux1}	40 Ω	R_{d1}	10 kΩ
R_{aux2}	10 Ω	R_{d2}	4.8 kΩ
S_{aux}	STW26NM60N	R_1 and R_2	9.1 kΩ
D_{aux}	F3C10065A	C_1	0.5 nF
Gate Driver	IR2110	C_2	1 nF
R_{H1}	1 MΩ	R_a	1 kΩ
R_b	2 kΩ		

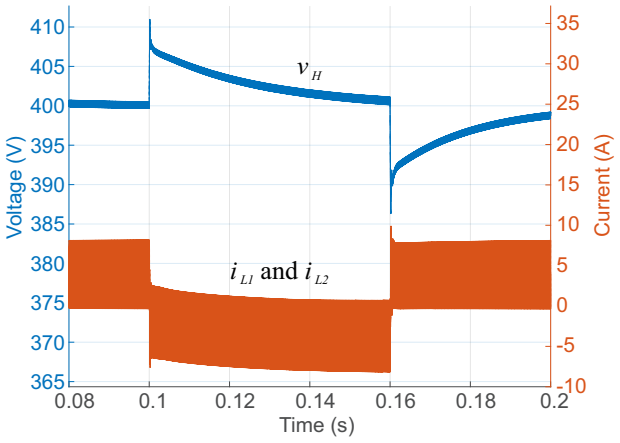

(a)

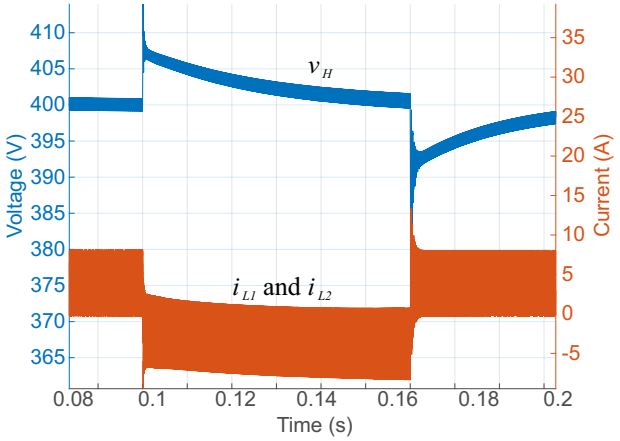

(b)

Fig. 10. Simulation results of power flux reversion. (a) Converter [26]. (b) Converter [27].

A. Power Flux Reversion

In Figures 11.a and 12.a is shown the experimental results of power flux reversion from step-up to step-down of the converters presented in Figure 6, while in Figures 11.b and 12.b is show the same, but for power flux reversion from step-down to step-up. Is notable that, the platform and its proposed control are worked well and the objective was achieved, proving the converters bidirectionality,once the zero crossing of the inductor current (i_{L1} and i_{L2}) has occurred while the voltage V_H has remained stable.

IX. CONCLUSIONS

With the growing of technologies that needs of power flux reversion, a several kind of bidirectional converters have been proposed, but the most part of these papers can not prove the online bidirectionality due the lack of information about how to do it. So, this paper present a new didactic technique to invert the power flux of bidirectional converter combining hardware and control techniques.Additionally, due the platform semiconductors present a natural clamping without resonance process, this platform can serve as a practical way to confirm the bidirectional operation of any bidirectional converter, as long as the current and voltage parameters of the semiconductors are respected.

Moreover, the simulation and experimental results

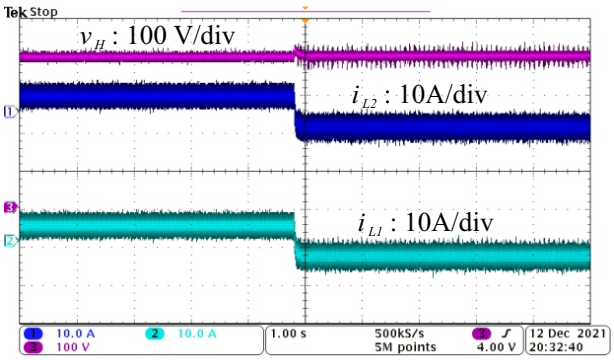

(a)

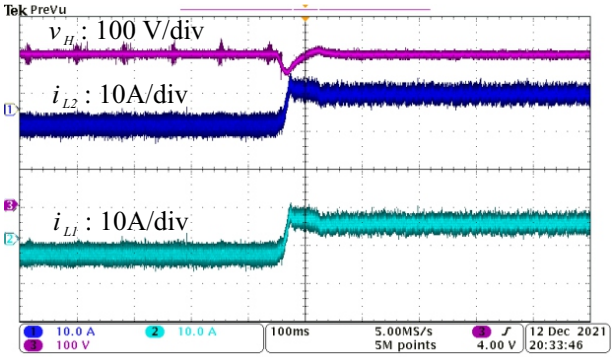

(b)

Fig. 11. Converter [26] power flux reversion from (a) Step-up to Step-down. (b) Step-down to Step-up.

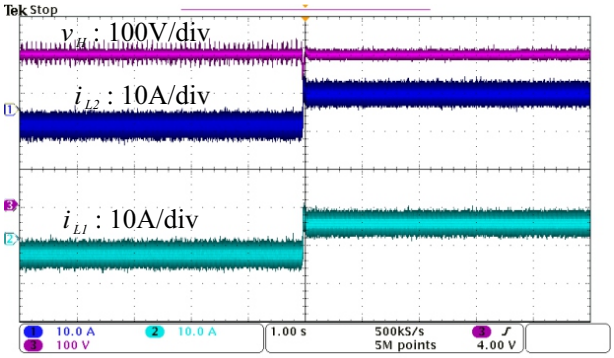

(a)

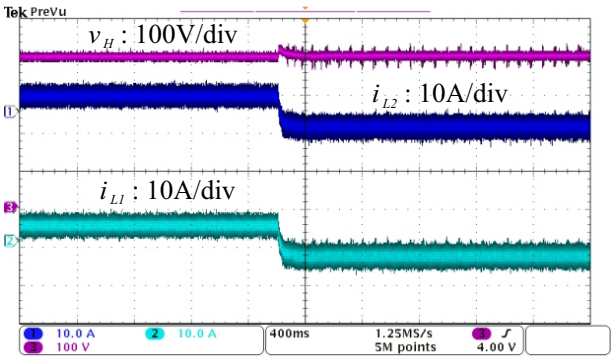

(b)

Fig. 12. Converter [27] power flux reversion from (a) Step-up to Step-down. (b) Step-down to Step-up.

presented highlight the good performance of the platform, as evidenced by the zero crossing of the inductors' current, without affecting the output voltage. This way, proving that the proposed platform can be used to extract power flux inversion results and hence prove the converter's bidirectionality. Besides that, this platforms is cheap and there is no need of expensive bidirectional power supplies to operate it.

ACKNOWLEDGEMENTS

This study was financed in part by the Coordenação de Aperfeiçoamento de Pessoal de Nível Superior – Brasil (CAPES/PROEX) – Finance Code 001 and Conselho Nacional de Desenvolvimento Científico e Tecnológico (Finance Code 307468/2022-4).

REFERENCES

[1] S. L. Rani, V. V. R. Raju, "V2G and G2V Technology in Micro-Grid Using Bidirectional Charger: A Review", *in Second International Conference on Power, Control and Computing Technologies (ICPC2T)*, pp. 1–5, 2022, doi: 10.1109/ICPC2T53885.2022.9777085.

[2] H. Fatima, M. T. Altaf, M. Jamil, "Power conditioning from EVs using bidirectional chargers: A Review", *in International Conference on Power, Instrumentation, Energy and Control (PIECON)*, pp. 1–5, 2023, doi: 10.1109/PIECON56912.2023.10085838.

[3] R. K. Kanaparthi, J. P. Singh, M. S. Ballal, "A Review on Multi-Port Bidirectional Isolated and Non-Isolated DC-DC Converters for Renewable Applications", *in IEEE International Conference on Power Electronics, Drives and Energy Systems (PEDES)*, pp. 1–6, 2022, doi:10.1109/PEDES56012.2022.10080049.

[4] Q. Lin, F. Cai, W. Wang, S. Chen, Z. Zhang, S. You, "A High-Performance Online Uninterruptible Power Supply (UPS) System Based on Multitask Decomposition", *IEEE Transactions on Industry Applications*, vol. 55, no. 6, pp. 7575–7585, Nov.–Dec. 2019, doi:10.1109/TIA.2019.2935929.

[5] K. Schwenk, S. Meisenbacher, B. Briegel, T. Harr, V. Hagenmeyer, R. Mikut, "Integrating Battery Aging in the Optimization for Bidirectional Charging of Electric Vehicles", *IEEE Transactions on Smart Grid*, vol. 12, no. 6, pp. 5135–5145, Nov. 2021, doi:10.1109/TSG.2021.3099206.

[6] M. Kumar, "Development of Control Strategies for Operation of Cluster of Interconnected Hybrid Microgrids in Islanded Mode", *IEEE Systems Journal*, vol. 17, no. 2, pp. 1741–1752, Jun. 2023, doi:10.1109/JSYST.2023.3239738.

[7] Z. Xie, L. Teng, Y. Yin, J. Liang, "Synchronous Switch Energy Extraction Circuit for Motor Regenerative Braking Enhancement", *IEEE Transactions on Circuits and Systems II: Express Briefs*, vol. 70, no. 5, pp. 1779–1783, May 2023, doi:10.1109/TCSII.2023.3254807.

[8] C. A. Arbugeri, N. C. Dal Pont, T. K. Jappe, S. A. Mussa, T. B. Lazzarin, "Control system for multi-inverter parallel operation in uninterruptible power systems", *Eletrônica de Potência (impresso)*, vol. 24, no. 1, pp. 37–46, Mar. 2019, doi:http://dx.doi.org/10.18618/REP.2019.1.0016.

[9] L. Michels, H. A. Gründling, "Procedimento de Projeto de Controladores Repetitivos para o Estágio de Saída de Fontes Ininterruptas de Energia", *Eletrônica de Potência (impresso)*, vol. 10, no. 1, pp. 39 – 50, Jun. 2005, doi:http://dx.doi.org/10.18618/REP.2005.1.039050.

[10] R. Mayer, M. B. E. Kattel, S. V. G. Oliveira, "Bidirectional DC-DC Converter with Coupled Inductor for DC-BUS Regulation in Microgrid Applications", *Eletrônica de Potência (impresso)*, vol. 25, no. 3, pp. 241–248, Sept. 2020, doi: http://dx.doi.org/10.18618/REP.2020.3.0007.

[11] G. M. de Souza Azevedo, M. C. Cavalcant, F. de Assis dos Santos Neves, L. R. Limongi, F. Bradaschia, "Microgrid Power Converter Control with Smooth Transient Response During the Change of Connection Mode", *Eletrônica de Potência (impresso)*, vol. 19, no. 3, pp. 285 – 294, Aug. 2014, doi:http://dx.doi.org/10.18618/REP.2014.3.285294.

[12] F. G. Nimitti, A. Manuel Santos Spencer Andrade, "Study About Architecture Classification of Bidirectional Non-Isolated Power Converters", *in 14th Seminar on Power Electronics and Control (SEPOC)*, pp. 1–5, 2022, doi: 10.1109/SEPOC54972.2022.9976429.

[13] F. G. Nimitti, J. C. Giacomini, A. M. S. S. Andrade, "Dual-Stacked Bidirectional Boost/Buck DC–DC Converter", *IEEE Transactions on Industrial Electronics*, vol. 70, no. 9, pp. 8873–8882, Sept. 2023, doi:10.1109/TIE.2022.3206756.

[14] F. G. Nimitti, M. M. da Silva, A. M. Santos Spencer Andrade, "Family of Bidirectional Boost/Buck DC-DC Converter", *in Brazilian Power Electronics Conference (COBEP)*, pp. 1–6, 2021, doi:10.1109/COBEP53665.2021.9684095.

[15] E. V. de Souza, I. Barbi, "Bidirectional flyback-push-pull DC-DC converter", *Eletrônica de Potência (impresso)*, vol. 20, no. 2, pp. 195–204, May 2015, doi: http://dx.doi.org/10.18618/REP.2015.2.195204.

[16] P. He, A. Khaligh, "Comprehensive Analyses and Comparison of 1 kW Isolated DC–DC Converters for Bidirectional EV Charging Systems", *IEEE Transactions on Transportation Electrification*, vol. 3, no. 1, pp. 147–156, Mar. 2017, doi:10.1109/TTE.2016.2630927.

[17] M. B. E. Kattel, R. Mayer, M. D. Possamai, S. V. G. Oliveirai, "Conversor CC-CC bidirecional push-pull/flyback", *Eletrônica de Potência (impresso)*, vol. 24, no. 1, pp. 85–94, Mar. 2019, doi:http://dx.doi.org/10.18618/REP.2019.1.0020.

[18] D. Meneses, O. García, P. Alou, J. A. Oliver, R. Prieto, J. A. Cobos, "Single-stage grid-connected forward microinverter with constant off-time boundary mode control", *in Twenty-Seventh Annual IEEE Applied Power Electronics Conference and Exposition (APEC)*, pp. 568–574, 2012, doi:10.1109/APEC.2012.6165876.

[19] E. A. Vendrusculo, A. A. Ferreira, J. A. Pomilio, "Plataforma Didática para Avaliação Rápida e Experimental de Estratégias de Controle em Eletrônica de Potência", *Eletrônica de Potência (impresso)*, vol. 13, no. 2, pp. 99–108, May 2008, doi:http://dx.doi.org/10.18618/REP.2008.2.099108.

[20] N. G. Bonacorso, V. Noll, B. de Melo Gevaerd, "Desenvolvimento de um Driver de Corrente Didático para Acionamento de Motores de Passo Aplicados ao Ensino de Eletrônica de Potência e Mecatrônica", *Eletrônica de Potência (impresso)*, vol. 13, no. 2, pp. 117–123, May 2008, doi:http://dx.doi.org/10.18618/REP.2008.2.117123.

[21] J. A. Pomilio, "Atividades Didáticas Experimentais em Eletrônica de Potência: Convergindo Conhecimentos e Tecnologias", *Eletrônica de Potência (impresso)*, vol. 25, no. 2, pp. 146–153, Jun. 2020, doi:http://dx.doi.org/10.18618/REP.2020.2.0023.

[22] B. S. Dupczak, "Protótipos Didáticos para o Ensino dos Conversores CC-CC", *Eletrônica de Potência (impresso)*, vol. 27, no. 3, pp. 244–253, Sept. 2022, doi:http://dx.doi.org/10.18618/REP.2022.3.0033.

[23] J. V. G. França, J. H. D. G. Pinto, D. do Carmo Mendonça, J. V. M. Farias, R. O. de Sousa, H. A. Pereira, S. I. S. Júnior, A. F. Cupertino, "Development of a Didactic Platform for Flexible Power Electronic Converters", *Eletrônica de Potência (impresso)*, vol. 27, no. 3, pp. 225–235, Sept. 2022, doi:http://dx.doi.org/10.18618/REP.2022.3.0012.

[24] R. R. S. da S. Vieira, F. G. Pereira, "Kit Didático de Transmissão de Veículos Híbridos", *Eletrônica de Potência (impresso)*, vol. 28, no. 1, pp. 36–41, Mar. 2023, doi:http://dx.doi.org/10.18618/REP.2023.1.0028.

[25] R. W. Erickson, D. Maksimović, *Fundamentals of Power Electronics*, third ed., Springer Cham, Switzerland, 2020.

[26] F. G. Nimitti, A. M. S. S. Andrade, "Analysis and Development of a Non-Isolated Bidirectional Converter Basead on Boost/Buck DC-DC Converter.", *Eletrônica de Potência (impresso)*, vol. 27, pp. 325–334, Dec. 2022, doi:http://dx.doi.org/10.18618/rep.2022.4.0006.

[27] F. G. Nimitti, A. M. S. S. Andrade, "Bidirectional converter based on boost/buck DC-DC converter for microgrids energy storage systems interface", *International Journal of Circuit Theory and Applications*, vol. 50, no. 12, pp. 4376–4394, Dec. 2022, doi:https://doi.org/10.1002/cta.3403.

[28] P. O. dos Reis Soares, *Discretização de Controladores Contínuos*, Master's thesis, University of Porto, Porto, 1996.

[29] A. Pertence, *Amplificadores Operacionais e Filtros Ativos*, 8ª ed., Bookman, 2015.

BIOGRAPHIES

Fabiano Gonzales Nimitti, received a Bachelor's degree in Electrical Engineering in 2020 from the Lutheran University of Brazil, Canoas, Brazil, and a Master's degree in Electrical Engineering in 2022 from the Federal University of Santa Maria, Santa Maria, Brazil. Currently, he is working toward the Ph.D. in Electrical Engineering at the Federal University of Santa Maria. His research interests include modular systems, modulation, power electronics control, and techniques of artificial intelligence applied to control systems. Fabiano has been a member of SOBRAEP since 2022.

António Manuel Santos Spencer Andrade, was born in Ribeira Grande, Cabo Verde, in 1989. He received his Bachelor's degree in Automation and Control Engineering from the University of Caxias do Sul, Caxias do Sul, Brazil, in 2012, and his Master's and Ph.D. degrees in Electrical Engineering from the Federal University of Santa Maria, Santa Maria, Brazil, in 2015 and 2018, respectively. Since 2018, he has been a professor at UFSM. He serves as an Associate Editor for the International Journal of Circuit Theory and Applications and Applied Sciences in the special edition "Renewable and Sustainable Energy Conversion Systems." He was also selected as a Distinguished Reviewer for 2020 by the IEEE Transactions on Power Electronics. His research interests include renewable energy, energy storage systems, DC-DC converters, and microinverters. Dr. António is a member of SOBRAEP and several IEEE societies.